NEURAL REGENERATION RESEARCH
July 2017, Volume 12, Issue 7
www.nrronline.org

RESEARCH ARTICLE

Dual face of axonal inhibitory inputs in the modulation of neuronal excitability in cortical pyramidal neurons

Lei Jiang[1, 2], **Hong Ni**[1], **Qi-yi Wang**[3], **Li Huang**[1], **Shi-di Zhao**[1], **Jian-dong Yu**[4], **Rong-jing Ge**[1, *]
1 Department of Pathophysiology, Bengbu Medical College, Bengbu, Anhui Province, China
2 Department of General Surgery, The Second Affiliated Hospital of Bengbu Medical College, Bengbu, Anhui Province, China
3 Department of Physiology, Bengbu Medical College, Bengbu, Anhui Province, China
4 Guangdong-Hongkong-Macau Institute of CNS Regeneration, Joint International Research Laboratory of CNS Regeneration, Ministry of Education, Jinan University, Guangzhou, Guangdong Province, China

How to cite this article: *Jiang L, Ni H, Wang QY, Huang L, Zhao SD, Yu JD, Ge RJ (2017) Dual face of axonal inhibitory inputs in the modulation of neuronal excitability in cortical pyramidal neurons. Neural Regen Res 12(7):1079-1085.*
Funding: *This study was supported by the National Natural Science Foundation of China, No. 31500836, 81671288; the Natural Science Foundation of Anhui Province of China, No. 1608085QH176.*

Graphical Abstract

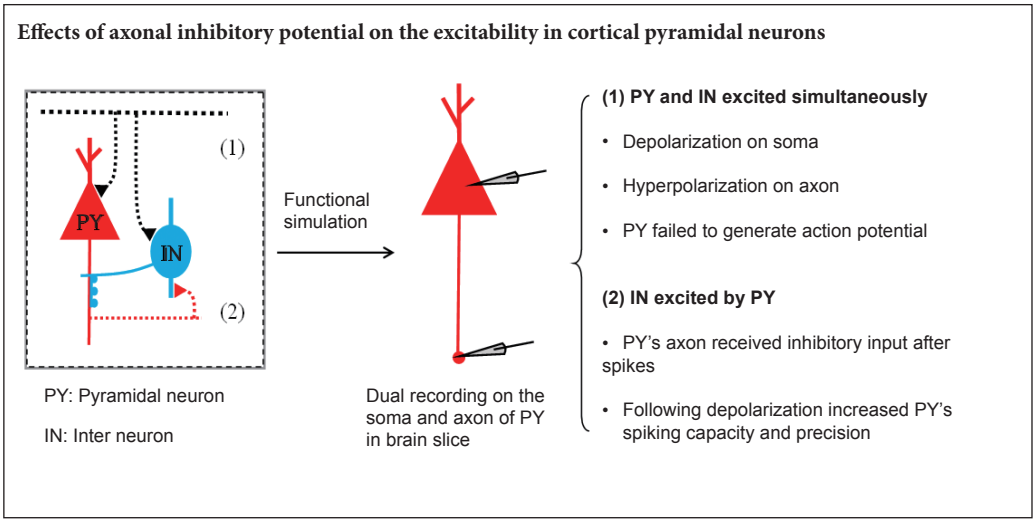

Correspondence to:
Rong-jing Ge, M.D., Ph.D., cathy0471@163.com.

orcid:
0000-0002-8633-7004 (Rong-jing Ge)

doi: *10.4103/1673-5374.211186*

Accepted: *2017-06-07*

Abstract

Limited by the tiny structure of axons, the effects of these axonal hyperpolarizing inputs on neuronal activity have not been directly elucidated. Here, we imitated these processes by simultaneously recording the activities of the somas and proximal axons of cortical pyramidal neurons. We found that spikes and subthreshold potentials propagate between somas and axons with high fidelity. Furthermore, inhibitory inputs on axons have opposite effects on neuronal activity according to their temporal integration with upstream signals. Concurrent with somatic depolarization, inhibitory inputs on axons decrease neuronal excitability and impede spike generation. In addition, following action potentials, inhibitory inputs on an axon increase neuronal spike capacity and improve spike precision. These results indicate that inhibitory inputs on proximal axons have dual regulatory functions in neuronal activity (suppression or facilitation) according to neuronal network patterns.

Key Words: *nerve regeneration; cortex; pyramidal neuron; soma; axon; hyperpolarization; neuronal network; feedforward inhibition; temporal integration; feedback inhibition; excitability; neural regeneration*

Introduction

The axon is a long process extending from the cell body of a neuron to the terminal, and is the main structure responsible for neuronal signal conduction. Numerous studies have focused on axonal function (Chen et al., 2010; Debanne et al., 2011; Grubb et al., 2011; Harty et al., 2013; Sasaki, 2013; Gulledge and Bravo, 2016; Whalley, 2016). Axons transmit both spikes and analog signals with high fidelity (Cross and Robertson, 2016). With a high density of sodium channels, the axon initial segment is a common onset point for action potentials (Kole et al., 2008; Kole and Stuart, 2008; Yu et al., 2010; Cross and Robertson, 2016). However, a sustained depolarizing current induces fewer spikes in an axon than in the soma, while in contrast, oscillation waves induce a higher frequency of spikes in the axon (Ge et al., 2011, 2014; Apostolides et al., 2016). Therefore, axons appear to have dif-

ferent responses to varied input patterns.

Additionally, receptors have been found on axons, especially on the axon initial segment and axon terminal (Sasaki et al., 2011; Trussell and Bender, 2012; Wefelmeyer et al., 2015; Gao and Heldt, 2016; Kerti-Szigeti and Nusser, 2016; Yin et al., 2017). Activation of these receptors leads to orthodromic propagation of the neuronal signal to axon terminals, which then influence subsequent neurotransmitter release (Sasaki et al., 2011). Field potentials from axon terminals also antidromically propagate back toward the soma, which can change the threshold for initiating action potentials (Paradiso and Wu, 2009). However, the roles of these receptors on proximal axons are still not clear. Structural studies have indicated that chandelier neurons, a subtype of GABAergic interneuron, have abundant projections that end on the proximal axons of pyramidal neurons in the cortex (Somogyi, 1977; Christie and De Blas, 2003; Taniguchi et al., 2013; Inan and Anderson, 2014).

These inhibitory axo-axonic synapses may have different effects on the output of pyramidal neurons according to the patterns of connections between interneurons and pyramidal neurons. To test this hypothesis, we conducted paired whole-cell recordings on the somas and proximal axons of pyramidal neurons in the cortex. We found that both spikes and subthreshold potentials propagated between somas and axons with high fidelity. Hyperpolarizing potentials on axons had entirely different effects on neuronal outputs depending on their temporal integration with upstream depolarization. These characteristics may play important roles in feedforward and feedback inhibitory circuits.

Materials and Methods

Animals

Twelve specific-pathogen-free male FVB/N mice at postnatal day 15–20, irrespective of sex, were enrolled in this study. This study and all experiments were fully approved by the Institutional Committee of Animal Care Unit in the Beijing Administration Office of Laboratory Animals (approval No. B10831). Surgeries were performed under anesthesia, and all possible efforts were made to minimize suffering.

The study protocol was approved by the Institutional Committee of Animal Care Unit in the Beijing Administration Office of Laboratory Animals (approval No. B10831). The experimental procedure followed the United States National Institutes of Health Guide for the Care and Use of Laboratory Animal (NIH Publication No. 85-23, revised 1986), and "Consensus Author Guidelines on Animal Ethics and Welfare" produced by the International Association for Veterinary Editors (IAVE).

Brain slices

Slices from sensory cortex (300 μm) were prepared from FVB mice. Postnatal day 15–20 mice were anesthetized with an injection of chloral hydrate (300 mg/kg) and decapitated with a guillotine. The cortical slices were cut with a vibratome in modified and oxygenized (95% O_2/5% CO_2) artificial cerebrospinal fluid (124 mM NaCl, 3 mM KCl, 1.2 mM NaH_2PO_4, 26 mM $NaHCO_3$, 0.5 mM $CaCl_2$, 5 mM $MgSO_4$, 10 mM dextrose, and 5 mM hydroxyethyl piperazine ethanesulfonic acid; pH 7.35) (Sinopharm Chemical Reagent Co., Ltd., Beijing, China) at 4°C and were then maintained in normal oxygenated artificial cerebrospinal fluid (126 mM NaCl, 2.5 mM KCl, 1.25 mM NaH_2PO_4, 26 mM $NaHCO_3$, 2.0 mM $CaCl_2$, 2.0 mM $MgSO_4$, and 25 mM glucose; pH 7.35) at 35°C for 1 hour before the experiments. A slice was transferred to a submersion chamber (Warner RC-26G, Molecular Devices, CA, USA) that was perfused with normal artificial cerebrospinal fluid for electrophysiological experiments (Ge et al., 2011, 2014).

Dual recording

We simultaneously recorded from somas and axonal blebs (Hu et al., 2009; Hu and Shu, 2012) of identical pyramidal cells in layers IV–V of cerebral cortex (MultiClapm-700B, Molecular Devices, CA, USA) under a fluorescent/DIC microscope (Nikon FN-E600). We differentiated between xonal blebs and dendritic blebs based on the process diameter and number of branches, as well as the polarity of neurons (Chen et al., 2010; Ge et al., 2014). Neuronal processes with fewer branches and fine diameters were categorized as axons. The electrical signals were input into a patch clamp (pClamp-10, Molecular Devices); the sampling rate was 50 kHz.

We confirmed that recordings were from two sites on the same neuron based on the presence of direct and corresponding electrical signals. Transient capacitance was compensated and the output bandwidth was 3 kHz. The pipette solution contained 150 mM K-gluconate, 5 mM NaCl, 0.4 mM ethylenebis (oxyethylenenitrilo) tetraacetic acid, 4 mM Mg-ATP, 0.5 mM Tris-GTP, 4 mM Na-phosphocreatine, and 5 hydroxyethyl piperazine ethanesulfonic acid (pH 7.4 adjusted by 2 M KOH) (Sinopharm Chemical Reagent Co., Ltd.). The osmolarity of the freshly made pipette solution was 295–305 mOsmol, and the pipette resistance was 10–15 MΩ.

Notably, pyramidal neuron axonal blebs formed from resealing the ends of cut axons during slice preparation. Although this preparation could be judged as an injured axon, several lines of evidence have indicated that axonal blebs are functionally intact. In axonal blebs, the resting membrane potential and action potential values are close to normal (Ge et al., 2011, 2014). Moreover, other immunohistochemical and electrophysiological study has suggested that the functions of axonal blebs are likely normal (Hu et al., 2009).

Capacity and timing precision (spike programming) are represented as the interspike interval and the standard deviation of spike timing, respectively (Guan et al., 2006; Wang et al., 2009). Data were analyzed if the recorded neurons had resting membrane potentials less than –60 mV. Additionally, data were excluded unless the changes in resting membrane potential, spike magnitude, and input resistance throughout each experiment were all less than 5%. Input resistance was monitored by measuring cell responses to hyperpolarization pulses at the same values as the depolarization that evoked spikes.

Statistical analysis

Data are presented as the mean ± SEM. All data were analyzed using SPSS 12.0 software (SPSS, Chicago, IL, USA). The parametric tests (unpaired *t*-test) were applied when normality (and homogeneity of variance) assumptions were satisfied. Otherwise, the equivalent non-parametric tests were used (Mann-Whitney *U* test). *P* values less than 0.05 were considered statistically significant.

Results

Signal transmission between somas and axons

We first determined whether subthreshold potentials or sequential spikes were transmitted from somas to axons with high fidelity. In whole-cell recordings of the soma and axonal bleb (**Figure 1A**), subthreshold analog current and long-term square pulses were injected into somas. The subthreshold analog current induced a subthreshold potential in the soma, and the same membrane oscillation was recorded in the axon (**Figure 1B**). The subthreshold analog signal was reliably transmitted from the soma to the axon (both in pattern and magnitude). Then, a long-term depolarizing pulse was injected into the soma to induce sequential spikes (upper panel in **Figure 1C**). In axonal recordings, corresponding spikes were recorded at almost the same time (lower panel in **Figure 1C**).

Critically, subthreshold waves and sequential spikes were also faithfully propagated from the axon to the soma. With the same recording pattern as that in **Figure 1**, input pulses were injected into the axonal bleb and somatic responses were recorded (**Figure 2**). We observed that subthreshold analog waves induced membrane potential oscillations in axons (lower panel in **Figure 2B**). Simultaneously, a similar wave was recorded in the soma (upper panel in **Figure 2B**). Sequential spikes were induced by injecting long-term depolarizing pulse into axonal blebs (lower panel in **Figure 2C**). Corresponding sequential spikes were recorded simultaneously in the soma (upper panel in **Figure 2C**). Interestingly, although the same current was injected into the soma and axons, the spiking patterns were different (compare **Figures 1C** and **2C**).

Axonal hyperpolarization impeded spike generation when the neuron is depolarized

With soma-axon paired recordings (**Figure 3A**), we investigated the effects of axonal activity on neuronal output. A short depolarizing current was injected into the soma to evoke a spike (upper panel in **Figure 3B**), without any axonal input, and the induced spike was transmitted to the axon (lower panel in **Figure 3B**). Then, we repeated the same procedure, but added a hyperpolarizing pulse (with the same intensity of the depolarizing current) applied to the axon. We found that for this combination, the pulse given to the soma failed to evoke an action potential (**Figure 3C**). Thus, when inhibitory potentials arrive at axons at the same time as upstream depolarization, neuronal excitability is reduced.

Subsequent hyperpolarization increased spike capacity and timing precision

Interspike interval (an index of spike capacity) and the standard deviation of spike timing (an index of spike timing precision) were measured by evoking sequential spikes with depolarizing currents (Wang et al., 2009). **Figure 4A** illustrates a repeat recording of sequential spikes in the soma. Spike intervals increase during sequential spiking, which represents greater spike capacity. However, spikes also drifted, especially during the latter part, which represents reduced spike precision.

Then, in addition to initial depolarizing current, short hyperpolarizing currents were injected into the soma following each spike. The result was a greater number of spikes within the same duration and more accurate spike firing (**Figure 4B**). Therefore, this subsequent hyperpolarization decreased interspike interval and improved spike timing precision. The first interspike interval values for corresponding spikes in these two groups did not differ significantly (unpaired *t*-test, $n = 6$, $P = 0.37$, $t = 0.94$, $df = 10$), but the second ones did (unpaired *t*-test, $n1 = 6$, $n2 = 6$, $P = 0.02$, $t = 2.83$, $df = 10$). Similarly, the first standard deviation of spike-timing values for corresponding spikes did not differ significantly between these two groups (unpaired *t*-test, $n1 = 6$, $n2 = 6$, $P = 0.45$, $t = 0.79$, $df = 10$), but the second ones did (unpaired *t*-test, $n = 6$, $P = 0.01$, $t = 3.01$, $df = 10$).

Subsequent hyperpolarization significantly increased spike capacity and spike precision in the axon. The same long-term depolarizing pulse as depicted in **Figure 4A** failed to induce sequential spikes in the axon (**Figure 5A**), and the later spikes drifted across a wide range. These results indicate that axons have poor firing rates and low accuracy following long-term depolarizing pulses.

Figure 5B shows that subsequent hyperpolarization following each spike markedly increased axonal spike capacity and spike precision. The interspike interval values for spike1 differed significantly between these two groups (unpaired *t*-test, $n1 = 6$, $n2 = 7$, $P = 0.02$, $t = 2.81$, $df = 9$), as did the values for spike2 (Mann-Whitney *U* test, $P = 0.03$, $u = 3$). Although the first standard deviation of spike-timing values for corresponding spikes did not differ significantly between these two groups (unpaired *t*-test, $P = 0.70$, $t = 0.40$, $df = 11$), the second ones did (Mann-Whitney *U* test, $P = 0.04$, $u = 7$).

Discussion

Numerous studies on the subcellular components of neurons have gradually identified elaborate structures and functions (Grubb and Burrone, 2010; Sheffield et al., 2011; Dugladze et al., 2012; Trussell and Bender, 2012). A growing number of studies have found that axons are not limited to propagating information downstream. Synaptic structures, which are mostly inhibitory, have been found in axons (Inan and Anderson, 2014; Kerti-Szigeti and Nusser, 2016; Kubota et al., 2016). In addition to dendritic input, synaptic input directly onto axons likely has a significant influence on neuronal output. The present study was designed to determine the effects of these axo-axonic inhibitory synapses on neuronal output. Regarding propagation, we found that action potentials and analog waves are faithfully propagated on axons (both orthodromically and antidromically). The most interesting finding

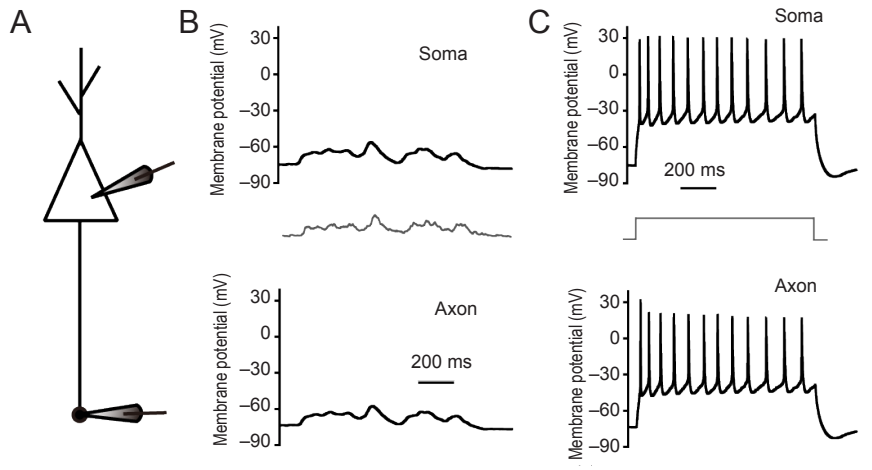

(A) Diagram of paired whole-cell recording at the soma (triangle) and the axon (lower black line) of the same pyramidal neuron in the cortex. The axonal recording was carried out on the axon bleb (black dot), which is a structure formed during slice incubation. (B) Subthreshold analog currents were injected into the soma, and corresponding potentials were recorded at the soma (upper panel, the waves come from another *in vivo* recording). At almost the same time, similar potentials were recorded at the axon (lower panel). (C) Long-term square-wave current was injected into the soma to induce spikes. A regular pattern of spikes was recorded at the soma (upper panel). Meanwhile, spikes with the same pattern were recorded at the axon (lower panel). These results were repeated in all 10 neurons tested.

Figure 1 Subthreshold potentials and spikes propagate from somas to axons with high fidelity.

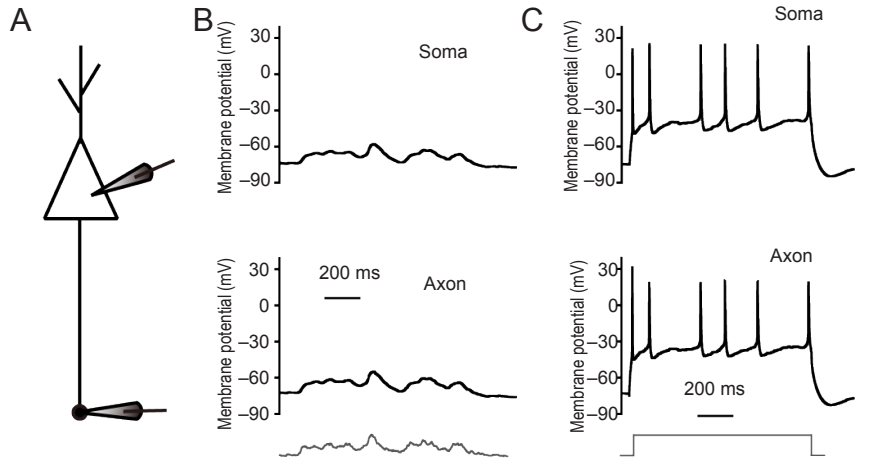

(A) Diagram of the same recording setup as in Experiment 1. (B) Subthreshold analog currents were injected into the axon, and corresponding potentials were recorded in the axon (upper panel, the waves come from another *in vivo* recording). Similar potentials were recorded in the soma at almost the same time. (C) Long-term square-wave current was injected into the axon to induce sequential spikes, which were fired in an irregular pattern (lower panel). Spikes with the same pattern were simultaneously recorded at the soma (upper panel). These results were repeated in all 10 neurons tested.

Figure 2 Subthreshold potentials and spikes propagate from axons to somas with high fidelity.

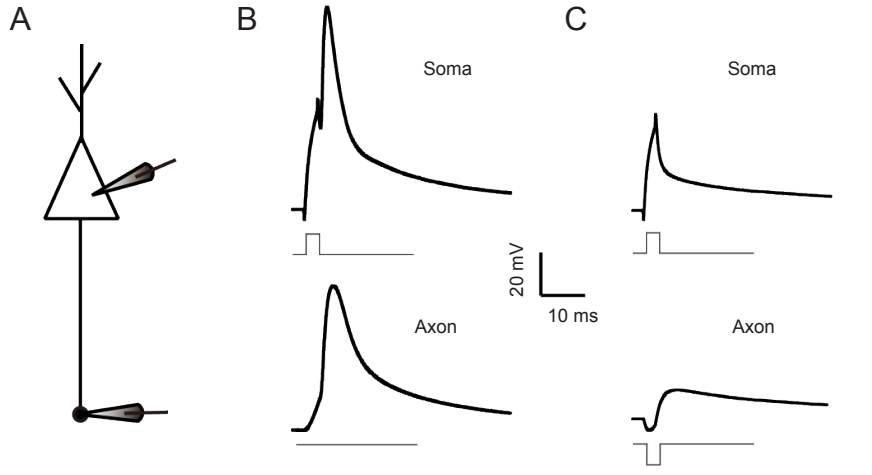

(A) Diagram of paired whole-cell recording at the soma (triangle) and the axon (lower black line) of the same pyramidal neuron in the cortex. (B) A short current (square pulse in middle panel) was injected into the soma to induce a spike without any axonal input (lower panel). The intensity of the somatic input current was adjusted to induce a spike. A spike was recorded both in somatic and axonal recordings. (C) The same depolarizing current in B was injected into the soma. Simultaneously, a hyperpolarizing current (with the same strength of the depolarizing current) was injected into the axon (lower panel). In this case, no spike was generated. These results were repeated in all 6 neurons tested.

Figure 3 Colliding with upstream depolarization, axonal hyperpolarization impeded spike generation.

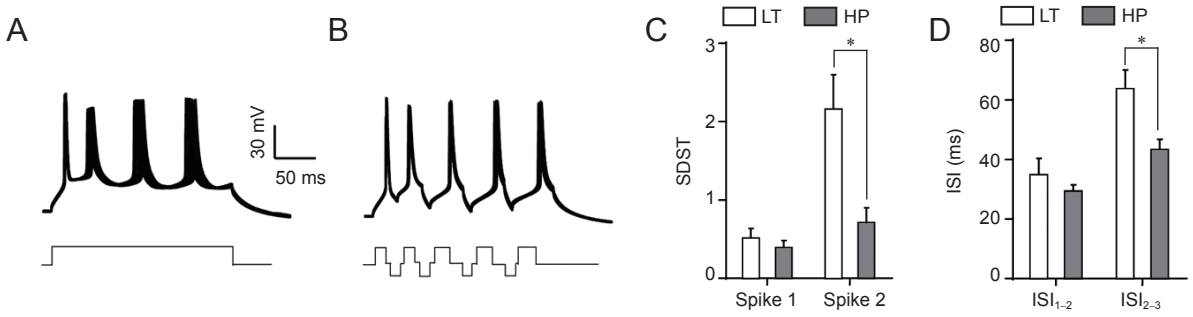

Figure 4 Subsequent hyperpolarization increases spike capacity and improves spike precision on the soma.
(A) Recording of sequential spikes at the soma when long-term depolarizing current was delivered to the soma. (B) Recording of sequential spikes at the soma when depolarizing current was delivered to the soma and hyperpolarizing currents were delivered following each spike. (C) Summary of the standard deviation of spike timing (SDST, which represents spike precision) for spike 1 and spike 2 induced by long-term depolarizing current in A and mixed currents in B. (D) Summary of the interspike intervals (ISI, which represents spike capacity) for ISI_{1-2} and ISI_{2-3} induced by LT and HP currents. Data are presented as the mean ± SEM ($n = 6$, unpaired t-test; $^*P < 0.05$). LT: Long-term depolarization; HP: hyperpolarization.

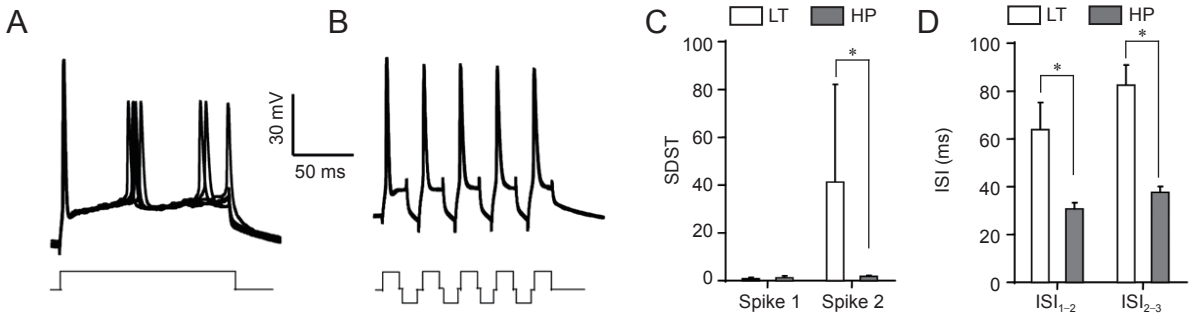

Figure 5 Subsequent hyperpolarization significantly increases spike capacity and improves spike precision on the axon.
(A) Recording of sequential spikes at the soma when long-term depolarizing current was delivered at the axon. (B) Recording of sequential spikes at the axon when hyperpolarizing currents were also delivered following each spike. (C) Summary of the standard deviation of spike timing (SDST, which represents spike precision) for spike 1 and spike 2 induced by LT and HP currents at the axon ($n1 = 6$, $n2 = 7$, unpaired t-test for spike1 and Mann-Whitney U test for spike2). (D) Summary of the interspike interval (ISI) for ISI_{1-2} and ISI_{2-3} induced by LT and HP currents at the axon. Data are presented as the mean ± SEM ($n1 = 6$, $n2 = 7$, unpaired t-test for ISI_{1-2} and Mann-Whitney U test for ISI2-3; $^*P < 0.05$). LT: Long-term depolarization; HP: hyperpolarization.

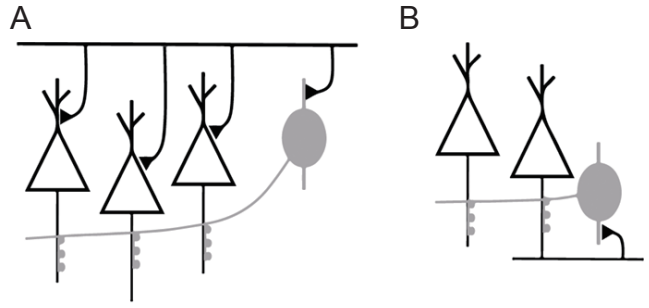

Figure 6 Diagrams of the sources for pyramidal axonal hyperpolarizing input.
(A) Feedforward inhibitory circuit formed by a pyramidal neuron and an interneuron (gray oval), which both receive upstream synaptic inputs. The axon of the interneuron projects to the proximal axons of several pyramidal neurons. Several synapses form on each pyramidal axon. In this circuit, the interneuron is excited at the same time as the pyramidal neurons (by the horizontal axon at the top). Thus, pyramidal neurons simultaneously receive upstream excitatory inputs and axonal inhibitory inputs. (B) Feedback inhibitory circuit formed by the pyramidal neuron and the downstream interneuron. The interneuron has back projections to the pyramidal neuron. In this circuit, the interneuron can be excited by pyramidal output and induce hyperpolarizing currents on the axon of the pyramidal neuron.

was that inhibitory input onto axons has opposite effects depending on how it is temporally integrated with upstream signals. When they coincide with upstream depolarization, inhibitory inputs on axons might impede the generation of action potentials. Following spikes, inhibitory inputs on axons can increase neuronal spike capacity and spike precision.

Subcellular propagation of subthreshold potentials and spikes

Subthreshold potentials can propagate significant distances along axons. Modest upstream changes propagate orthodromically toward the axon terminal to modulate neurotransmission (Cox et al., 2000; Shu et al., 2006). Additionally, the small potentials in nerve terminals back-propagate up the axon to influence spike generation (Paradiso and Wu, 2009). We observed both orthodromic and antidromic propagation of subthreshold voltage between somas and axons in our research. Furthermore, sequential spikes induced by long-term square pulses were also faithfully propagated between somas and axons. However, the sequential spikes induced at the soma have different patterns than those at axons. Compared with spikes induced on somas, spikes induced on axons are less frequent and more irregular. As mentioned in our previ-

ous study, sodium channels in axons are likely inactive and difficult to reactivate during sustained depolarization (Ge et al., 2014). Because of this, sustained depolarization on axons failed to induce regular sequential spikes.

Sources of axonal input and the effects on neuronal excitability

Receptors have been found along axons, especially in the proximal segment and the terminal end. Receptors on axonal terminals modulate local membrane excitability and neurotransmitter release (Starke et al., 1989; Herrero et al., 1992; Smirnova et al., 1993; Ohura and Kamiya, 2016). Spraying glutamate on an axon increases the width of an axon spike (Sasaki et al., 2011). Additionally, synapses have been found on axons, especially on the axon initial segment. These axo-axonic synapse are always GABAergic and innervated by chandelier neurons (Somogyi, 1977; Xia et al., 2014). Whether these GABAergic synapses on the axon initial segment have inhibitory or excitatory functions remains controversial (Szabadics et al., 2006; Woodruff and Yuste, 2008; Xia et al., 2014; Spampanato et al., 2016; Saha et al., 2017a, b).

Chandelier neurons are abundant in the cortex and form feedforward and feedback circuits with pyramidal neurons (Jang et al., 2005; Woodruff and Yuste, 2008; Inan and Anderson, 2014; Wang et al., 2016) (**Figure 6**). In the feedforward circuit, chandelier neurons are excited simultaneously with pyramidal neurons. At the same time, pyramidal neurons receive excitatory inputs *via* dendrites/soma and inhibitory inputs *via* the axon initial segment. Inhibitory inputs on the axon initial segment decrease the excitability of pyramidal neurons. This hyperpolarization decreases total injected current. Whether this hyperpolarized current changes the spiking threshold needs to be verified in future studies. In the feedback circuit, pyramidal neurons excite chandelier neurons. Consequently, pyramidal neurons receive inhibitory inputs from chandelier neurons on the axon initial segment. As we observed here, this subsequent hyperpolarization increases spike capacity and spike precision of pyramidal neurons. With these feedforward and feedback models, we found that inhibitory inputs on the axon initial segment have significantly different effects on neuronal excitability. Concurrent inhibitory inputs on the axon initial segment offset upstream excitatory inputs and impede spike generation. Spikes following inhibitory inputs promote subsequent spike generation. Previous work has shown that hyperpolarization after spiking can accelerate the reactivation of sodium channels (Chen et al., 2006).

Coordinated communication between neurons is essential for functional neuronal networks (Zhao et al., 2012; Zhao and Wang, 2014; Maris et al., 2016). Conversely, network activity modulates both the structure and activity of single neurons during development and regeneration. During neuronal regeneration, recovering of neural activity and signal propagation are important. This study provides an efficient method and informative results for the measurement of axonal function.

Conclusion

With paired recordings at somas and axons, we directly observed the effects of axonal inhibitory inputs on neuronal excitability. Varied temporal integration with upstream waves and inhibitory inputs on axons regulate neuronal excitability in different ways. These adjustments enrich the activities of neuronal networks.

Author contributions: *LJ, HN, QYW, LH, SDZ, JDY and RJG contributed to the experiments and data analyses. RJG contributed to project design and paper writing. All authors approved the final version of the paper.*
Conflicts of interest: *None declared.*
Research ethics: *The study protocol was approved by the Institutional Committee of Animal Care Unit in the Beijing Administration Office of Laboratory Animals (approval No. B10831). The experimental procedure followed the United States National Institutes of Health Guide for the Care and Use of Laboratory Animal (NIH Publication No. 85-23, revised 1986), and "Consensus Author Guidelines on Animal Ethics and Welfare" produced by the International Association for Veterinary Editors (IAVE). All efforts were made to minimize the number and suffering of animals used in this study. The article was prepared in accordance with the "Animal Research: Reporting of In Vivo Experiments Guidelines" (ARRIVE Guidelines).*

Contributor agreement: *A statement of "Publishing Agreement" has been signed by an authorized author on behalf of all authors prior to publication.*
Plagiarism check: *This paper has been checked twice with duplication-checking software iThenticate.*
Peer review: *A double-blind and stringent peer review process has been performed to ensure the integrity, quality and significance of this paper.*
Open peer review reports:
***Reviewer 1**: Jun Zhao, NIH, NIMH, USA.*
***Comments to the author:** The authors investigated how inhibitory inputs modulated axonal excitability in cortical pyramidal neurons with electrophysiological methods. They report opposite effects of inhibitory inputs on axonal signal transmission, which is an interesting and timely finding. The methodologies employed are fancy and sophisticated. The finding is potentially important to the clinic treatment in neural regeneration. Please see additional file for more details.*
Additional file: *Open peer review report 1.*
***Reviewer 2**: Panja Debabrata, USA.*
***Comments to the author:** This is a short article with only electrophysiology experiments and data, in the field of signal processing in the Axon Initial Segment (AIS). This article should be published with changes to the text with better explanation of the model system and the rational behind using the model (how the model mimics the real scenario of recording directly from AIS) to study the inhibitory GABAergic inputs to the AIS. The authors also need to improve the presentation of the data with a microscopic picture of the dual recordings rather than only a schematic diagram. Please see additional file for more details.*
Additional file: *Open peer review report 2.*

References

Apostolides PF, Milstein AD, Grienberger C, Bittner KC, Magee JC (2016) Axonal filtering allows reliable output during dendritic plateau-driven complex spiking in CA1 neurons. Neuron 89:770-783.
Chen N, Chen X, Yu J, Wang J (2006) Afterhyperpolarization improves spike programming through lowering threshold potentials and refractory periods mediated by voltage-gated sodium channels. Biochem Biophys Res Commun 346:938-945.
Chen N, Yu J, Qian H, Ge R, Wang JH (2010) Axons amplify somatic incomplete spikes into uniform amplitudes in mouse cortical pyramidal neurons. PLoS One 5:e11868.

Christie S, De Blas A (2003) GABAergic and glutamatergic axons innervate the axon initial segment and organize GABAA receptor clusters of cultured hippocampal pyramidal cells. J Comp Neurol 456:361-374.
Cox CL, Denk W, Tank DW, Svoboda K (2000) Action potentials reliably invade axonal arbors of rat neocortical neurons. Proc Natl Acad Sci U S A 97:9724-9728.
Cross KP, Robertson RM (2016) Ionic mechanisms maintaining action potential conduction velocity at high firing frequencies in an unmyelinated axon. Physiol Rep 4:e12814.
Debanne D, Campanac E, Bialowas A, Carlier E, Alcaraz G (2011) Axon physiology. Physiol Rev 91:555-602.
Dugladze T, Schmitz D, Whittington MA, Vida I, Gloveli T (2012) Segregation of axonal and somatic activity during fast network oscillations. Science 336:1458-1461.
Gao Y, Heldt SA (2016) Enrichment of GABAA receptor α-subunits on the axonal initial segment shows regional differences. Front Cell Neurosci 10:39.
Ge R, Qian H, Wang JH (2011) Physiological synaptic signals initiate sequential spikes at soma of cortical pyramidal neurons. Mol Brain 4:19.
Ge R, Qian H, Chen N, Wang JH (2014) Input-dependent subcellular localization of spike initiation between soma and axon at cortical pyramidal neurons. Mol Brain 7:26.
Grubb MS, Burrone J (2010) Building and maintaining the axon initial segment. Curr Opin Neurobiol 20:481-488.
Grubb MS, Shu Y, Kuba H, Rasband MN, Wimmer VC, Bender KJ (2011) Short-and long-term plasticity at the axon initial segment. J Neurosci 31:16049-16055.
Guan S, Ma S, Zhu Y, Ge R, Wang Q, Wang JH (2006) The intrinsic mechanisms underlying the maturation of programming sequential spikes at cerebellar Purkinje cells. Biochem Biophys Res Commun 345:175-180.
Gulledge AT, Bravo JJ (2016) Neuron morphology influences axon initial segment plasticity. eNeuro. doi: 10.1523/ENEURO.0085-15.
Harty RC, Kim TH, Thomas EA, Cardamone L, Jones NC, Petrou S, Wimmer VC (2013) Axon initial segment structural plasticity in animal models of genetic and acquired epilepsy. Epilepsy Res 105:272-279.
Herrero I, Miras-Portugal MT, Sánchez-Prieto J (1992) Positive feedback of glutamate exocytosis by metabotropic presynaptic receptor stimulation. Nature 360:163-166
Hu W, Shu Y (2012) Axonal bleb recording. Neurosci Bull 28:342-350.
Hu W, Tian C, Li T, Yang M, Hou H, Shu Y (2009) Distinct contributions of Nav1. 6 and Nav1. 2 in action potential initiation and backpropagation. Nat Neurosci 12:996-1002.
Inan M, Anderson SA (2014) The chandelier cell, form and function. Curr Opin Neurobiol 26:142-148.
Jang IS, Ito Y, Akaike N (2005) Feed-forward facilitation of glutamate release by presynaptic GABA A receptors. Neuroscience 135:737-748.
Kerti-Szigeti K, Nusser Z (2016) Similar GABAA receptor subunit composition in somatic and axon initial segment synapses of hippocampal pyramidal cells. Elife 5:e18426.
Kole M, Stuart G (2008) Is action potential threshold lowest in the axon? Nat Neurosci 11:1253-1255.
Kole M, Ilschner S, Kampa B, Williams S, Ruben P, Stuart G, Neuroscience N (2008) Action potential generation requires a high sodium channel density in the axon initial segment. Nature 200:8.
Kubota Y, Karube F, Nomura M, Kawaguchi Y (2016) The diversity of cortical inhibitory synapses. Front Neural Circuits 10:27.
Maris E, Fries P, van Ede F (2016) Diverse phase relations among neuronal rhythms and their potential function. Trends Neurosci 39:86-99.
Ohura S, Kamiya H (2016) Excitability tuning of axons in the central nervous system. J Physiol Sci 66:189-196.
Paradiso K, Wu L (2009) Small voltage changes at nerve terminals travel up axons to affect action potential initiation. Nat Neurosci 12:541-543.
Saha R, Knapp S, Chakraborty D, Kriebel M, Ehrlich I, Volkmer H, Richter-Levin G (2017a) GABAergic synapses at the axon initial segment of basolateral amygdala projection neuron modulate behavioral flexibility. Eur Neuropsychopharmacol 27:S28-29.
Saha R, Knapp S, Chakraborty D, Horovitz O, Albrecht A, Kriebel M, Kaphzan H, Ehrlich I, Volkmer H, Richter-Levin G (2017b) GABAergic synapses at the axon initial segment of basolateral amygdala projection neurons modulate fear extinction. Neuropsychopharmacology doi: 10.1038/npp.2016.205.
Sasaki T (2013) The axon as a unique computational unit in neurons. Neurosci Res 75:83-88.
Sasaki T, Matsuki N, Ikegaya Y (2011) Action-potential modulation during axonal conduction. Science 331:599.
Sheffield ME, Best TK, Mensh BD, Kath WL, Spruston N (2011) Slow integration leads to persistent action potential firing in distal axons of coupled interneurons. Nat Neurosci 14:200-207.
Shu Y, Hasenstaub A, Duque A, Yu Y, McCormick D (2006) Modulation of intracortical synaptic potentials by presynaptic somatic membrane potential. Nature 441:761-765.
Smirnova T, Stinnakre J, Mallet J (1993) Characterization of a presynaptic glutamate receptor. Science 262:430-433.
Somogyi P (1977) A specific 'axo-axonal'interneuron in the visual cortex of the rat. Brain Res 136:345-350.
Spampanato J, Sullivan RKP, Perumal MB, Sah P (2016) Development and physiology of GABAergic feedback excitation in parvalbumin expressing interneurons of the mouse basolateral amygdala. Physiol Rep doi: 10.14814/phy2.12664.
Starke K, Göthert M, Kilbinger H (1989) Modulation of neurotransmitter release by presynaptic autoreceptors. Physiol Rev 69:864-989.
Szabadics J, Varga C, Molnar G, Olah S, Barzo P, Tamas G (2006) Excitatory effect of GABAergic axo-axonic cells in cortical microcircuits. Science 311:233-235.
Taniguchi H, Lu J, Huang ZJ (2013) The spatial and temporal origin of chandelier cells in mouse neocortex. Science 339:70-74.
Trussell L, Bender KJ (2012) A new view of the axon initial segment. Ann Rev Neurosci 35:249-265.
Wang Q, Liu X, Ge R, Guan S, Zhu Y, Wang JH (2009) The postnatal development of intrinsic properties and spike encoding at cortical GABAergic neurons. Biochem Biophys Res Commun. 378:706-710.
Wang Y, Zhang P, Wyskiel DR (2016) Chandelier cells in functional and dysfunctional neural circuits. Front Neural Circuits 10:33.
Wefelmeyer W, Cattaert D, Burrone J (2015) Activity-dependent mismatch between axo-axonic synapses and the axon initial segment controls neuronal output. Proc Natl Acad Sci U S A 112:9757-9762.
Whalley K (2016) Neurophysiology: Local tuning of spike shape. Nat Rev Neurosci 17:466-466.
Woodruff A, Yuste R (2008) Of mice and men, and chandeliers. PLoS Biol 6:e243.
Xia Y, Zhao Y, Yang M, Zeng S, Shu Y (2014) Regulation of action potential waveforms by axonal gabaa receptors in cortical pyramidal neurons. PLoS One 9:e100968.
Yin L, Rasch MJ, He Q, Wu S, Dou F, Shu Y (2017) Selective modulation of axonal sodium channel subtypes by 5-HT1A receptor in cortical pyramidal neuron. Cereb Cortex 27:509-521.
Yu Y, Maureira C, Liu X, McCormick D (2010) P/Q and N channels control baseline and spike-triggered calcium levels in neocortical axons and synaptic boutons. J Neurosci 30:11858-11869.
Zhao J, Wang JH (2014) Whisker tactile adaptation is encoded by inactivity and asynchrony of network neurons and astrocytes in barrel cortex through ampar desensitization. Prog Biochem Biophys 41:804-817.
Zhao J, Wang D, Wang JH (2012) Barrel cortical neurons and astrocytes coordinately respond to an increased whisker stimulus frequency. Mol brain 5:12.

Copyedited by Wang J, Li CH, Qiu Y, Song LP, Zhao M